

Encyclopedia of emergent particles in type-IV magnetic space groups

Zeying Zhang,^{1,*} Gui-Bin Liu,^{2,3,*} Zhi-Ming Yu,^{2,3} Shengyuan A. Yang,⁴ and Yugui Yao^{2,3,†}

¹College of Mathematics and Physics, Beijing University of Chemical Technology, Beijing 100029, China

²Centre for Quantum Physics, Key Laboratory of Advanced Optoelectronic Quantum Architecture and Measurement (MOE), School of Physics, Beijing Institute of Technology, Beijing, 100081, China

³Beijing Key Lab of Nanophotonics & Ultrafine Optoelectronic Systems, School of Physics, Beijing Institute of Technology, Beijing, 100081, China

⁴Research Laboratory for Quantum Materials, Singapore University of Technology and Design, Singapore 487372, Singapore

The research on emergent particles in condensed matters has been attracting tremendous interest, and recently it is extended to magnetic systems. Here, we study the emergent particles stabilized by the symmetries of type-IV magnetic space groups (MSGs). Type-IV MSGs feature a special time reversal symmetry $\{\mathcal{T}|\mathbf{t}_0\}$, namely, the time reversal operation followed by a half lattice translation, which significantly alters the symmetry conditions for stabilizing the band degeneracies. In this work, based on symmetry analysis and modeling, we present a complete classification of emergent particles in type-IV MSGs by studying all possible (spinless and spinful, essential and accidental) particles in each of the 517 type-IV MSGs. Particularly, the detailed correspondence between the emergent particles and the type-IV MSGs that can host them are given in easily accessed interactive tables, where the basic information of the emergent particles, including the symmetry conditions, the effective Hamiltonian, the band dispersion and the topological characters can be found. According to the established encyclopedia, we find that several emergent particles that are previously believed to exist only in spinless systems will occur in spinful systems here, and vice versa, due to the $\{\mathcal{T}|\mathbf{t}_0\}$ symmetry. Our work not only deepens the understanding of the symmetry conditions for realizing emergent particles but also provides specific guidance for searching and designing materials with target particles.

Introduction. In crystals, the atoms are arranged in an orderly manner, forming crystal lattices extending in three directions in real space and leading to periodic band structure in momentum space [1]. The symmetries of the bare crystal lattice are described by the space groups, where all the operators can be made unitary. By further including the spin and orbital degrees of freedom in the crystal, anti-unitary operations such as time reversal and its combinations with certain spatial symmetries need to be considered, and the extension leads to the magnetic space groups. Correspondingly, the energy bands of crystals should be labeled by the corepresentation of the relevant MSG [2, 3].

With certain symmetry conditions, the energy bands may form degeneracies in the Brillouin zone (BZ), giving rise to topological semimetal states [4–16]. Because the degeneracies are singularities in momentum space, the excitations around the degeneracies show many novel and intriguing phenomena, such as chiral anomaly, quantum vortex, chiral Landau levels and divergent optical responses [16–26]. Hence the topological semimetals have been one of the most active research fields in the past ten years [27–31].

Rooted in the MSG symmetries and the corepresentations, the band degeneracies take diverse forms, and each kind of degeneracy can exhibit distinct properties [1, 32–37]. Thus, of fundamental importance to list and classify all possible band degeneracies, along with their

symmetry conditions. A complete classification of emergent particles in type-II and type-III MSGs have recently been presented by us in Ref. [38] and Ref. [39], respectively. Here, we complete the last missing piece of the project, i.e., the classification for the type-IV MSGs.

There are 517 type-IV MSGs, of which share the following structure

$$\mathbf{M} = \mathbf{G} + \{\mathcal{T}|\mathbf{t}_0\}\mathbf{G}, \quad (1)$$

where \mathbf{G} is a space group, \mathcal{T} is the time reversal operation, and \mathbf{t}_0 is a half lattice translation. The "shifted" time reversal operation $\{\mathcal{T}|\mathbf{t}_0\}$ connects two lattice sites with opposite magnetic moments, indicating that type-IV MSGs describe systems with certain antiferromagnetic orders. The appearance of $\{\mathcal{T}|\mathbf{t}_0\}$ is also reminiscent of nonsymmorphic symmetries, which are point group operations followed by a fractional lattice translation. Because of $\{\mathcal{T}|\mathbf{t}_0\}$, although the crystals belonging to type-IV MSG are magnetic systems without the pure \mathcal{T} symmetry, its energy band still exhibit the \mathcal{T} symmetry, reflected as $E_n(\mathbf{k}) = E_n(\mathcal{T}\mathbf{k})$. However, the $\{\mathcal{T}|\mathbf{t}_0\}$ here is quite different from the pure \mathcal{T} symmetry but similar to the nonsymmorphic spatial operators. The extra fractional translation may lead new possibilities of the emergent particles in type-IV MSGs. For example, consider the eight time-reversal invariant momenta (TRIMs) in spinless case, $\{\mathcal{T}|\mathbf{t}_0\}^2 = e^{-2i\mathbf{k}\cdot\mathbf{t}_0}$ will generate double degeneracy at TRIMs which satisfy $2\mathbf{k}\cdot\mathbf{t}_0 = \pi$. This is distinct from other space groups, where the pure \mathcal{T} symmetry can lead to the Kramers double degeneracy only for spinful systems.

In this work, we systematically study all the possible

* These two authors contribute equally to this work.

† ygyao@bit.edu.cn

TABLE I. The main results of the difference between type-IV magnetic space group and type-II MSG. “ \checkmark ” (“ \times ”) means there (do not) exist corresponding emergent particles in magnetic space groups. “II” and “IV” represent the type-II MSG and type-IV magnetic space group, respectively. The “ \checkmark ” with red color means that the emergent particles exist in type-IV magnetic space group but not exist in type-II MSG, and the “ \checkmark ” with green color means that the emergent particles exist in type-II MSG but not exist in type-IV magnetic space group. “Single (Double)” is for emergent particles with (without) SOC.

Notation	Abbr.	Single		Double		Notation	Abbr.	Single		Double	
		II	IV	II	IV			II	IV	II	IV
Charge-1 Weyl point	C-1 WP	\checkmark	\checkmark	\checkmark	\checkmark	Charge-2 Weyl point	C-2 WP	\checkmark	\checkmark	\checkmark	\checkmark
Charge-3 Weyl point	C-3 WP	\checkmark	\checkmark	\checkmark	\checkmark	Charge-4 Weyl point	C-4 WP	\checkmark	\checkmark	\times	\checkmark
Triple point	TP	\checkmark	\times	\checkmark	\times	Charge-2 triple point	C-2 TP	\checkmark	\checkmark	\checkmark	\checkmark
Quadratic triple point	QTP	\checkmark	\checkmark	\times	\times	Quadratic contact triple point	QCTP	\checkmark	\checkmark	\times	\times
Dirac point	DP	\checkmark	\checkmark	\checkmark	\checkmark	Charge-2 Dirac point	C-2 DP	\checkmark	\checkmark	\checkmark	\checkmark
Charge-4 Dirac point	C-4 DP	\times	\checkmark	\checkmark	\checkmark	Quadratic Dirac point	QDP	\checkmark	\checkmark	\checkmark	\checkmark
Charge-4 quadratic Dirac point	C-4 QDP	\times	\checkmark	\checkmark	\checkmark	Quadratic contact Dirac point	QCDP	\times	\times	\checkmark	\checkmark
Cubic Dirac point	CDP	\times	\times	\checkmark	\checkmark	Cubic crossing Dirac point	CCDP	\checkmark	\checkmark	\times	\times
Sextuple point	SP	\checkmark	\checkmark	\checkmark	\checkmark	Charge-4 sextuple point	C-4 SP	\times	\checkmark	\checkmark	\times
Quadratic contact sextuple point	QCSP	\times	\times	\checkmark	\times						
Octuple point	OP	\times	\times	\checkmark	\checkmark						
Weyl nodal line	WNL	\checkmark	\checkmark	\checkmark	\checkmark	Weyl nodal line (net)	WNLs	\checkmark	\checkmark	\checkmark	\checkmark
Quadratic nodal line	QNL	\checkmark	\checkmark	\checkmark	\checkmark	Cubic nodal line	CNL	\times	\times	\checkmark	\checkmark
Dirac nodal line	DNL	\checkmark	\checkmark	\checkmark	\checkmark	Dirac nodal line (net)	DNLs	\checkmark	\checkmark	\checkmark	\checkmark
Nodal surface	NS	\checkmark	\checkmark	\checkmark	\checkmark	Multiple nodal surfaces	NSs	\checkmark	\checkmark	\checkmark	\checkmark

emergent particles protected by the symmetries of type-IV MSGs, and classify the emergent particles from four aspects, namely, the dimension of degeneracy manifold, the degree of degeneracy, the type of dispersion, and the topological charge. The main results are shown in Table 1, where one can find most of the emergent particles (except QCSP) can be realized in type-IV MSGs. The corepresentation information and the possible emergent particles, including spinless and spinful, essential and accidental particles for each of the 517 type-IV MSGs are given in easily accessible interactive tables in S5 of Supplemental Material (SM). We also compare the differences between results of type-IV MSGs and that of type-II MSGs (nonmagnetic systems with pure \mathcal{T} symmetry) in table I. For type-II MSGs, the C-4 WP only appears in spinless systems while the C-4 DP, the C-4 QDP and the C-4 SP only appear in spinful systems [38]. In contrast, for type-IV MSGs the C-4 SP only appear in spinless systems, and the C-4 WP, the C-4 DP, and the C-4 QDP can appear in both spinless and spinful systems, due to the $\{\mathcal{T}|\mathbf{t}_0\}$ symmetry. We construct concrete lattice models to demonstrate the existence of C-4 WP in spinful systems and the existence of C-4 DP in spinless systems. Together with Ref. [38] and [39], our work accomplishes

the grand task of classifying all possible emergent particles in periodic lattices.

Rationale. To study the degeneracies stabilized by the symmetries of type-IV MSGs, we should obtain the corepresentation information of type-IV MSGs. The method to calculate the corepresentation information of type-IV MSGs are exactly same as that of type-II MSGs [1]. Specifically, the corepresentation of a type-IV MSG \mathbf{M} can be induced from the small corepresentations of $M_{\mathbf{k}}$, where $M_{\mathbf{k}}$ is the magnetic little group of \mathbf{k} in \mathbf{M} . This step is done by our homemade package MSGCorep [40]. With the calculated small corepresentation information of $M_{\mathbf{k}}$, we can easily identify the possible degeneracies protected by the symmetries of $M_{\mathbf{k}}$ and establish the $\mathbf{k} \cdot \mathbf{p}$ Hamiltonians expanded around the corresponding degeneracy. Many crucial properties of the degeneracies can be inferred from the $\mathbf{k} \cdot \mathbf{p}$ Hamiltonians, such as the dimension of degeneracy manifold, the type of band splitting, and the topological charge. A complete list of all possible emergent particles and their detailed classification is presented in S4 of SM, arranged for each of the 517 type-IV MSGs.

Compare with nonmagnetic systems. We also compare the particles in type-IV MSGs with that in type-II MSGs

TABLE II. Complex emergent particles existing in type-IV MSGs. The format of this table is similar to Tab. I

Notation	Abbr.	Single		Double		Notation	Abbr.	Single		Double	
		II	IV	II	IV			II	IV	II	IV
Combined WNL and NS	WNL/NS	✓	✓	✓	✓	Combined WNLs and NSs	WNLs/NSs	✓	✓	×	×
Combined QNL and NS	QNL/NS	×	✓	×	✓	Combined QNL and WNLs	QNL/WNLs	✓	✓	✓	✓
Combined QNLs and WNLs	QNLs/WNLs	✓	×	×	×	Combined CNL and NS	CNL/NS	×	×	×	✓
Combined CNL and WNLs	CNL/WNLs	×	×	×	✓						

(nonmagnetic systems), and the results are shown in table I. All kinds of accidental band degeneracies on high symmetry lines found in type-II MSGs can also be realized in type-IV MSGs. Hence, let's focus on the essential band degeneracies. First, a notable feature for type-IV MSGs is that the C-4 WP can exist in spinful systems. However, for nonmagnetic systems, the C-4 WP can only exist in spinless materials. Besides, the C-3 WP can appear as essential band crossing protected by the single type-IV MSGs, but it is only allowed as accidental band crossing on high symmetry line in type-II MSGs. Moreover, the C-4 DP, C-4 QDP and C-4 SP, emerged as spinful particles in nonmagnetic can exist in spinless systems belonging to type-IV MSGs.

Second, there are more possibilities of the complex particles in type-IV MSGs. Here the complex emergent particles refer to the degeneracies that include two or multiple different kinds of particles and these particles share one same degenerate point in BZ. For example, the complex particle CNL/NS in MSG 184.196 includes a CNL residing along ΓA line and a NS located at AHL plane, and the CNL and NS are connected at joint point of A . However, such CNL/NS complex particle cannot be realized in type-II MSGs. Besides, the complex particles of QNL/NS, CNL/NS and CNL/WNLs can appear in type-IV MSGs but can not occur at type-II MSGs, as shown in Table II.

C-4 WP and C-4 DP. According to previously results, the C-4 WP and C-4 DP only exist in spinless and spinful systems respectively for type-II MSGs. However, the $\{\mathcal{T}|t_0\}$ symmetry brings new possibilities, making the realization of C-4 WP in spinful systems and that of C-4 DP in spinless systems. According to our classification [see S4C of SM], we find that the C-4 WP can be realized in the magnetic materials with SOC effect at the R point of MSG 198.11, 212.62 and 213.66. Here, we use a concrete spinful lattice model with MSG 198.11 to demonstrate the existence of C-4 WP. Part of the result in SM for MSG 198.11 are shown in table III. In this table, we present many important properties of MSG 198.11, including the information of the corresponding BZ, the corepresentation information of each high-symmetry momentum, and the possible degeneracies protected by the MSG symmetries.

There are four points which need to be clarified, (i) for the spinful cases with IT symmetry, all bands are at least doubly degenerate in the whole Brillouin zone due to the

Kramers degeneracy ($(IT)^2 \equiv -1$) and for spinless cases with IT , one can always choose the proper basis to obtain a real Hamiltonian, then the degeneracy manifold for doubly degenerate point in those cases are always large than 0, i.e. the degenerate point is on a nodal line or NS [11]. (ii) The blue text in S5 of SM (marked as Greek letters and Latin capital letters) are clickable. One can directly click them to get the full form of corepresentation matrices and Hamiltonians. (iii) In order to avoid redundant data in S7 of SM, the Hamiltonian marked as $H_n^{R_i}$ which means the expression of Hamiltonian is exactly the same as the Hamiltonian in R_i corepresentation of magnetic space group n , despite their corepresentation matrices may different. (iv) The symmetry operations for magnetic space groups are taken from Bradley and Cracknell's (BC) book [1]. However, some magnetic space groups are mistaken in the BC book, which are not consistent with their BNS notations [2, 3]. These magnetic space groups are corrected in the package MSGCorep [40], and hence all magnetic space groups we used here are consistent with those used in Bilbao Crystallographic Server or ISOTROPY [41, 42].

For the spinful systems with MSG 198.11, one has $\{\mathcal{T}|t_0\}^2 = -1$ for Γ , M and $\{\mathcal{T}|t_0\}^2 = 1$ for R , X , as $t_0 = (\frac{1}{2}\frac{1}{2}\frac{1}{2})$. Hence, the band in Γ and M must at least be doubly degenerate, while in R and X do not have such constraints. The generators of corepresentation matrices for R_5R_6 of R point can be written as

$$\begin{aligned}
D(\{C_{2z}|\frac{1}{2}0\frac{1}{2}\}) &= -D(\{C_{2x}|\frac{1}{2}\frac{1}{2}0\}) = \sigma_0 \\
D(\{C_{3z}|000\}) &= \gamma\sigma_{19} = -\frac{1}{2}\sigma_0 - i\frac{\sqrt{3}}{2}\sigma_3 \\
D(\{\mathcal{T}|\frac{1}{2}\frac{1}{2}\frac{1}{2}\}) &= \sigma_1
\end{aligned} \tag{2}$$

where the definition of σ_i and γ can be found in S6 of SM. Then the $\mathbf{k}\cdot\mathbf{p}$ Hamiltonian at R point can be solved from the constraint equations

$$H(\mathbf{k}) = \begin{cases} D(Q)H(R^{-1}\mathbf{k})D^{-1}(Q) & \text{if } Q = \{R|\mathbf{t}\} \\ D(Q)H^*(-R^{-1}\mathbf{k})D^{-1}(Q) & \text{if } Q = \{RT|\mathbf{t}\} \end{cases} \tag{3}$$

where $D(Q)$ is the corepresentation matrices for symmetry operation Q with rotation part R and translation part

t . The $\mathbf{k} \cdot \mathbf{p}$ Hamiltonian for R_5R_6 is [43]

$$H = (c_1 + c_2k^2) \sigma_0 + c_5k_xk_yk_z\sigma_3 + (c_3k_x^2 + c_4k_y^2 - c_3k_z^2 - c_4k_x^2) \sigma_1 + \frac{\sqrt{3}}{3} (c_3k^2 - 3c_3k_y^2 - c_4k^2 + 3c_4k_x^2) \sigma_2 \quad (4)$$

where $k^2 = k_x^2 + k_y^2 + k_z^2$. Such Hamiltonian host (223)

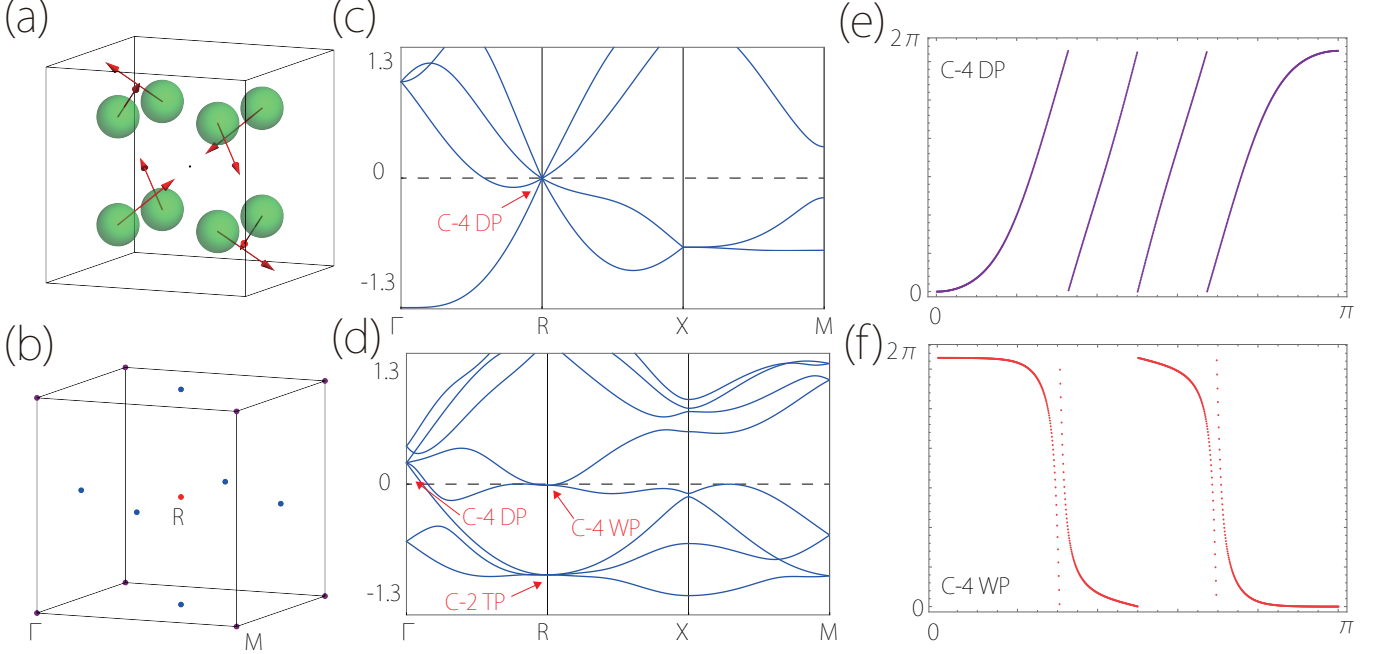


FIG. 1. (a)Structure of lattice model. (b)Schematic showing the C-4 WP C-4 DP and C-1 WPs in Brillouin zone, the red, purple and blue points represent C-4 WP, C-4 DP and C-1 WPs, receptively. (c-d) Band structure of lattice models without SOC(c) and with SOC(d). (e-f) Wilson loop of C-4 DP and C-4 WP located at Γ (e) and R (f) and the horizontal coordinates are polar angle θ of the sphere.

To further confirm our results, we construct both spinless and spinful lattice models for MSG 198.11. Notice the minimum Wyckoff position of 198.11 is $8a$, consider the $|\phi_s\rangle$ (spinless) and $\{|\phi_s \uparrow\rangle, |\phi_s \downarrow\rangle\}$ (spinful) for each atom in $8a$. Then we can construct two tight-binding models (see S2 of SM for Hamiltonian and parameters) [44]. The structure for active atom of the lattice model is shown in Fig. 1. Moreover, for spinful case there are another C-4 DP locate at Γ as show in Fig. 1(b) The calculated band structure of this twos models are plotted in

Fig. 1(c-d). The topological charge for emergent particles can be obtained by calculating the Wilson loops on a sphere enclosing the WP (DP)

$$W(\theta) = \oint d\mathbf{k} \langle \psi(\mathbf{k}) | i\nabla | \psi(\mathbf{k}) \rangle \quad (5)$$

where θ is the polar angle of the sphere. The integration is over an enclosing loop of a constant polar angle of the sphere. The evolution of Wilson loop for Γ and R with considering SOC are shown in Fig. 1(e-f) which are consist with table III.

TABLE III: Part of the emergent particles in type-IV magnetic space group 198.11. The text above the double line of table are the basic information of magnetic space group, including the symbol of magnetic space group, the Bravais lattice, the generators of the magnetic space group, whether exist the combination of inversion symmetry (I) and \mathcal{T} , and whether SOC is considered. The column for \mathbf{k} show the name and coordinate of high-symmetry momenta [1]. The column for “generators” is the rotation part for generators of magnetic little group of \mathbf{k} . The column for “corep” is the information of corepresentation of \mathbf{k} ’s magnetic little group, including the label, dimension and corepresentation matrices for generators. The last three column are the $\mathbf{k} \cdot \mathbf{p}$ Hamiltonian, type of emergent particles and topological charge respectively.

198.11, P_12_13

Γ_c , $\{C_{2z}|\frac{1}{2}0\frac{1}{2}\}$, $\{C_{2x}|\frac{1}{2}\frac{1}{2}0\}$, $\{C_{31}^+|000\}$, $\{\mathcal{T}|\frac{1}{2}\frac{1}{2}\frac{1}{2}\}$, without IT

\mathbf{k}		generators	corep			$\mathbf{k} \cdot \mathbf{p}$ Hamiltonian	node type	\mathcal{C}
name	kinfo		label	dim	matrices			
Spinless emergent particles								
Γ	000	$C_{2z}, C_{2x}, C_{31}^+, \mathcal{T}$	$\Gamma_2\Gamma_3$	2	$\sigma_0, \sigma_0, -\gamma\sigma_{19}, \sigma_1$	$H_{195.3}^{\Gamma_2\Gamma_3}$	C-4 WP	4
			Γ_4	3	$-A_{37}, A_{18}, A_9, A_0$	$H_{195.3}^{\Gamma_4}$	C-2 TP	2
X	$0\frac{1}{2}0$	$C_{2x}, C_{2y}, \mathcal{T}$	X_1	2	$-\sigma_1, \sigma_4, \sigma_4$	$H_{18.22}^{Y_1}$	C-1 WP	1
R	$\frac{1}{2}\frac{1}{2}\frac{1}{2}$	$C_{2z}, C_{2x}, C_{31}^+, \mathcal{T}$	R_1	2	$-i\sigma_3, i\sigma_1, -\delta\sigma_{25}, \sigma_4$	$H_{195.3}^{\Gamma_5}$	C-1 WP	1
			R_2R_3	4	$-i\Gamma_{50}, i\Gamma_{30}, \eta\Gamma_{92}, -\Gamma_{13}$	$H_{195.3}^{\Gamma_6\Gamma_7}$	C-4 DP	4
Spinful emergent particles								
Γ	000	$C_{2z}, C_{2x}, C_{31}^+, \mathcal{T}$	Γ_5	2	$-i\sigma_3, -i\sigma_1, \delta\sigma_{25}, \sigma_4$	$H_{195.3}^{\Gamma_5}$	C-1 WP	1
			$\Gamma_6\Gamma_7$	4	$-i\Gamma_{50}, -i\Gamma_{30}, -\eta\Gamma_{92}, -\Gamma_{13}$	$H_{195.3}^{\Gamma_6\Gamma_7}$	C-4 DP	4
M	$\frac{1}{2}\frac{1}{2}0$	$C_{2x}, C_{2y}, \mathcal{T}$	M_5	2	$\sigma_1, -i\sigma_4, \sigma_4$	$H_{18.22}^{Y_1}$	C-1 WP	1
R	$\frac{1}{2}\frac{1}{2}\frac{1}{2}$	$C_{2z}, C_{2x}, C_{31}^+, \mathcal{T}$	R_5R_6	2	$\sigma_0, -\sigma_0, \gamma\sigma_{19}, \sigma_1$	$H_{195.3}^{\Gamma_2\Gamma_3}$	C-4 WP	4
			R_7	3	$A_{18}, A_{37}, -A_{12}, A_0$	$H_{198.11}^{R_7}$	C-2 TP	2

Discussion and conclusion. In this work, we have theoretically listed the emergent particles in type-IV magnetic space groups. However, It remains an important task to identify realistic materials that can host these emergent particles. To put it into practice, one can directly look up our tables in S5 of SM to find the possible emergent particles by the MSG number in the material database [45–47]. Besides, S4 of SM also shows in which MSGs the specific emergent particles can exist. Experimentally, the spinful emergent particles can be directly probed by the angle-resolved photoemission spectroscopy (ARPES) method [48]. It can also break the \mathcal{T} symmetry in artificial systems, which make it possible to detect spinless emergent particles in type-IV MSGs, e.g., the \mathcal{T} breaking photonic crystals can be realized by assembling magnetic rods [49, 50]. The physical properties such as the magnetoresponse, transport behavior, topological surface states and magneto-optical effect for emergent particles in type-IV magnetic space group still need further investigation. For example, the large surface density of states for magnetic higher-order nodal lines might be beneficial for realizing surface magnetism and surface high-temperature superconductivity [35].

In conclusion, with the powerful tool—group represen-

tation theory, we establish the encyclopedia of emergent particles in type-IV magnetic space groups which can provides useful guidance to search and study magnetic topological materials. Two interesting directions for the future are: (i) investigate the emergent particles in spin-space groups which have decoupled spin and lattice symmetries, (ii) use compatibility relations to study the connectivity of energy bands and the coexistence of emergent particles for specific Wyckoff position.

Acknowledgments. This work is supported by the NSF of China (Grants Nos. 12004028, 12004035, 11734003, 12061131002), the China Postdoctoral Science Foundation (Grant No. 2020M670106), the Strategic Priority Research Program of Chinese Academy of Sciences (Grant No. XDB30000000), the National Key R&D Program of China (Grant No. 2020YFA0308800), , the Beijing Natural Science Foundation (Grant No. Z190006) and the Singapore MOE AcRF Tier 2 (Grant No. MOE2019-T2-1-001).

Note added. During completion of our paper, two independent and complementary works with a list of $\mathbf{k} \cdot \mathbf{p}$ Hamiltonians for 1651 magnetic space groups appeared in Ref. [51, 52]. **The SM of this manuscript can be found in zipped tar source file (TYPE-IV-EP-SM.pdf).**

- [1] C. Bradley and A. Cracknell, *Mathematical theory of symmetry in solids: representation theory for point groups and space groups* (OUP, Oxford, 2009).
- [2] N. V. Belov, N. N. Neronova, and T. S. Smirnova, 1651 shubnikov groups, *Sov. Phys. Crystallogr* **1**, 487 (1957).
- [3] N. V. Belov, N. N. Neronova, and T. S. Smirnova, Shubnikov groups, *Sov. Phys. Crystallogr* **2**, 311 (1957).
- [4] L. Michel and J. Zak, Connectivity of energy bands in crystals, *Physical Review B* **59**, 5998 (1999).
- [5] A. A. Burkov, M. D. Hook, and L. Balents, Topological nodal semimetals, *Physical Review B* **84**, 235126 (2011).
- [6] X. Wan, A. M. Turner, A. Vishwanath, and S. Y.

Savrasov, Topological semimetal and Fermi-arc surface states in the electronic structure of pyrochlore iridates, *Phys. Rev. B* **83**, 205101 (2011).

- [7] C. Fang, M. J. Gilbert, X. Dai, and B. A. Bernevig, Multi-Weyl Topological Semimetals Stabilized by Point Group Symmetry, *Phys. Rev. Lett.* **108**, 266802 (2012).
- [8] B.-J. Yang and N. Nagaosa, Classification of stable three-dimensional Dirac semimetals with nontrivial topology, *Nature Communications* **5**, ncomms5898 (2014).
- [9] B. Lv, H. Weng, B. Fu, X. Wang, H. Miao, J. Ma, P. Richard, X. Huang, L. Zhao, G. Chen, Z. Fang, X. Dai, T. Qian, and H. Ding, Experimental Discovery of Weyl

- Semimetal TaAs, *Physical Review X* **5**, 031013 (2015).
- [10] S. M. Young and C. L. Kane, Dirac Semimetals in Two Dimensions, *Physical Review Letters* **115**, 126803 (2015).
- [11] H. Huang, J. Liu, D. Vanderbilt, and W. Duan, Topological nodal-line semimetals in alkaline-earth stannides, germanides, and silicides, *Physical Review B* **93**, 201114(R) (2016).
- [12] B. Bradlyn, J. Cano, Z. Wang, M. G. Vergniory, C. Felser, R. J. Cava, and B. A. Bernevig, Beyond Dirac and Weyl fermions: Unconventional quasiparticles in conventional crystals, *Science* **353**, aaf5037 (2016).
- [13] T. Bzdušek, Q. Wu, A. Rüegg, M. Sgrist, and A. A. Soluyanov, Nodal-chain metals, *Nature* **538**, 75 (2016).
- [14] Z. Yan, R. Bi, H. Shen, L. Lu, S.-C. Zhang, and Z. Wang, Nodal-link semimetals, *Physical Review B* **96**, 041103(R) (2017).
- [15] W. Wu, Y. Liu, S. Li, C. Zhong, Z.-M. Yu, X.-L. Sheng, Y. X. Zhao, and S. A. Yang, Nodal surface semimetals: Theory and material realization, *Physical Review B* **97**, 115125 (2018).
- [16] Z.-M. Yu, W. Wu, X.-L. Sheng, Y. X. Zhao, and S. A. Yang, Quadratic and cubic nodal lines stabilized by crystalline symmetry, *Physical Review B* **99**, 121106(R) (2019).
- [17] A. A. Zyuzin and A. A. Burkov, Topological response in Weyl semimetals and the chiral anomaly, *Physical Review B* **86**, 115133 (2012).
- [18] A. Burkov, Chiral Anomaly and Diffusive Magnetotransport in Weyl Metals, *Physical Review Letters* **113**, 247203 (2014).
- [19] X. Huang, L. Zhao, Y. Long, P. Wang, D. Chen, Z. Yang, H. Liang, M. Xue, H. Weng, Z. Fang, X. Dai, and G. Chen, Observation of the Chiral-Anomaly-Induced Negative Magnetoresistance in 3D Weyl Semimetal TaAs, *Physical Review X* **5**, 031023 (2015).
- [20] T. Morimoto, S. Zhong, J. Orenstein, and J. E. Moore, Semiclassical theory of nonlinear magneto-optical responses with applications to topological Dirac/Weyl semimetals, *Physical Review B* **94**, 245121 (2016).
- [21] M. Hirschberger, S. Kushwaha, Z. Wang, Q. Gibson, S. Liang, C. Belvin, B. Bernevig, R. Cava, and N. Ong, The chiral anomaly and thermopower of Weyl fermions in the half-Heusler GdPtBi, *Nature Materials* **15**, 1161 (2016).
- [22] T. Liu, M. Franz, and S. Fujimoto, Quantum oscillations and Dirac-Landau levels in Weyl superconductors, *Physical Review B* **96**, 224518 (2017).
- [23] J. E. Moore, Optical properties of Weyl semimetals, *National Science Review* **6**, 206 (2019).
- [24] Y. Okamura, S. Minami, Y. Kato, Y. Fujishiro, Y. Kaneko, J. Ikeda, J. Muramoto, R. Kaneko, K. Ueda, V. Kocsis, N. Kanazawa, Y. Taguchi, T. Koretsune, K. Fujiwara, A. Tsukazaki, R. Arita, Y. Tokura, and Y. Takahashi, Giant magneto-optical responses in magnetic Weyl semimetal Co₃Sn₂S₂, *Nature Communications* **11**, 4619 (2020).
- [25] X. Yuan, C. Zhang, Y. Zhang, Z. Yan, T. Lyu, M. Zhang, Z. Li, C. Song, M. Zhao, P. Leng, M. Ozerov, X. Chen, N. Wang, Y. Shi, H. Yan, and F. Xiu, The discovery of dynamic chiral anomaly in a Weyl semimetal NbAs, *Nature Communications* **11**, 1259 (2020).
- [26] Z. Song, J. Zhao, Z. Fang, and X. Dai, Detecting the chiral magnetic effect by lattice dynamics in Weyl semimetals, *Physical Review B* **94**, 214306 (2016).
- [27] M. Z. Hasan and C. L. Kane, Colloquium: Topological insulators, *Reviews of Modern Physics* **82**, 3045 (2010).
- [28] B. Bradlyn, L. Elcoro, J. Cano, M. G. Vergniory, Z. Wang, C. Felser, M. I. Aroyo, and B. A. Bernevig, Topological quantum chemistry, *Nature* **547**, 298 (2017).
- [29] N. P. Armitage, E. J. Mele, and A. Vishwanath, Weyl and Dirac semimetals in three-dimensional solids, *Reviews of Modern Physics* **90**, 015001 (2018).
- [30] C.-K. Chiu, J. C. Teo, A. P. Schnyder, and S. Ryu, Classification of topological quantum matter with symmetries, *Reviews of Modern Physics* **88**, 035005 (2016).
- [31] H. C. Po, A. Vishwanath, and H. Watanabe, Symmetry-based indicators of band topology in the 230 space groups, *Nature Communications* **8**, 931 (2017).
- [32] C. J. Bradley and B. L. Davies, Magnetic Groups and Their Corepresentations, *Reviews of Modern Physics* **40**, 359 (1968).
- [33] R.-X. Zhang and C.-X. Liu, Topological magnetic crystalline insulators and corepresentation theory, *Physical Review B* **91**, 115317 (2015).
- [34] H. Watanabe, H. C. Po, and A. Vishwanath, Structure and topology of band structures in the 1651 magnetic space groups, *Science Advances* **4**, eaat8685 (2018).
- [35] Z. Zhang, Z.-M. Yu, and S. A. Yang, Magnetic higher-order nodal lines, *Physical Review B* **103**, 115112 (2021).
- [36] L. Elcoro, B. J. Wieder, Z. Song, Y. Xu, B. Bradlyn, and B. A. Bernevig, Magnetic topological quantum chemistry, *Nature Communications* **12**, 5965 (2021).
- [37] J. Wang, Antiferromagnetic topological nodal line semimetals, *Physical Review B* **96**, 081107 (2017).
- [38] Z.-M. Yu, Z. Zhang, G.-B. Liu, W. Wu, X.-P. Li, R.-W. Zhang, S. A. Yang, and Y. Yao, Encyclopedia of emergent particles in three-dimensional crystals, *Science Bulletin* **10.1016/j.scib.2021.10.023** (2021).
- [39] Encyclopedia of emergent particles in three-dimensional crystals. II. Quasiparticles in type-III magnetic space groups, [arxiv:2111.04372](https://arxiv.org/abs/2111.04372) (2021).
- [40] G.-B. Liu and et al., MSGCorep: A package for corepresentations of magnetic space groups, to be published., (2021).
- [41] M. I. Aroyo, A. Kirov, C. Capillas, J. M. Perez-Mato, and H. Wondratschek, Bilbao Crystallographic Server. II. Representations of crystallographic point groups and space groups, *Acta Crystallographica Section A* **62**, 115 (2006).
- [42] ISOTROPY Software Suite, <https://iso.byu.edu/>.
- [43] Z. Zhang and et al., MagneticKP: A package for kp model of magnetic and non-magnetic materials, to be published., (2021).
- [44] Z. Zhang, Z.-M. Yu, G.-B. Liu, and Y. Yao, MagneticTB: A package for tight-binding model of magnetic and non-magnetic materials, *Computer Physics Communications* **270**, 108153 (2022).
- [45] S. Curtarolo, W. Setyawan, S. Wang, J. Xue, K. Yang, R. H. Taylor, L. J. Nelson, G. L. Hart, S. Sanvito, M. Buongiorno-Nardelli, N. Mingo, and O. Levy, AFLOWLIB.ORG: A distributed materials properties repository from high-throughput ab initio calculations, *Computational Materials Science* **58**, 227 (2012).
- [46] S. V. Gallego, J. M. Perez-Mato, L. Elcoro, E. S. Tasci, R. M. Hanson, K. Momma, M. I. Aroyo, and G. Madariaga, MAGNDATA: towards a database of magnetic structures. I. The commensurate case, *Journal of Applied Crystallography* **49**, 1750 (2016).

- [47] A. Jain, S. P. Ong, G. Hautier, W. Chen, W. D. Richards, S. Dacek, S. Cholia, D. Gunter, D. Skinner, G. Ceder, and K. A. Persson, Commentary: The Materials Project: A materials genome approach to accelerating materials innovation, *APL Materials* **1**, 011002 (2013).
- [48] B. Lv, T. Qian, and H. Ding, Angle-resolved photoemission spectroscopy and its application to topological materials, *Nature Reviews Physics* **1**, 609 (2019).
- [49] Z. Wang, Y. Chong, J. D. Joannopoulos, and M. Soljačić, Observation of unidirectional backscattering-immune topological electromagnetic states, *Nature* **461**, 772 (2009).
- [50] L. Lu, C. Fang, L. Fu, S. G. Johnson, J. D. Joannopoulos, and M. Soljačić, Symmetry-protected topological photonic crystal in three dimensions, *Nature Physics* **12**, 337 (2016).
- [51] F. Tang and X. Wan, Exhaustive construction of effective models in 1651 magnetic space groups, *Physical Review B* **104**, 085137 (2021).
- [52] Y. Jiang, Z. Fang, and C. Fang, A kp Effective Hamiltonian Generator, *Chin. Phys. Lett.* **38**, 077104 (2021).